J|A|C|S
ARTICLES
Published on Web 07/23/2003

Synthesis, Structure, and Activity of Enhanced Initiators for Olefin Metathesis

Jennifer A. Love, Melanie S. Sanford, Michael W. Day, and Robert H. Grubbs*

Contribution from the Arnold and Mabel Beckman Laboratories for Chemical Synthesis, Division of Chemistry and Chemical Engineering, California Institute of Technology, Pasadena, California 91125

Received June 26, 2002

Abstract: A series of ruthenium olefin metathesis catalysts of the general structure $(H_2IMes)(PR_3)(Cl)_2Ru{=}CHPh$ (H_2IMes = 1,3-dimesityl-4,5-dihydroimidazol-2-ylidene) have been prepared; these complexes are readily accessible in two steps from commercially available $(H_2IMes)(PCy_3)(Cl)_2Ru{=}CHPh$. Their phosphine dissociation rate constants (k_1), relative rates of phosphine reassociation, and relative reaction rates in ring-opening metathesis polymerization (ROMP) and ring-closing metathesis (RCM) have been investigated. The rates of phosphine dissociation (initiation) from these complexes increase with decreasing phosphine donor strength. Complexes containing a triarylphosphine exhibit dramatically improved initiation relative to $(H_2IMes)(PCy_3)(Cl)_2Ru{=}CHPh$. Conversely, phosphine reassociation shows no direct correlation with phosphine electronics. In general, increased phosphine dissociation leads to faster olefin metathesis reaction rates, which is of direct significance to both organic and polymer metathesis processes.

Introduction

Olefin metathesis has become a widely used reaction in organic and polymer chemistry.[1] Key to the utility of this reaction has been the emergence of commercially available catalysts **1**−**3** (Figure 1). Whereas the ruthenium-based complex **1**[2] has greater functional group compatibility than the molybdenum-based complex **3**, **3** exhibits greater reactivity, particularly with sterically demanding and electron-deficient olefins.[3] The development of *N*-heterocyclic carbenes (NHC) as ligands for ruthenium closed the gap between the molybdenum and ruthenium systems.[4] These ruthenium-based complexes, such as **2**, have similar reactivity to the molybdenum complexes while maintaining the high functional group tolerance and air and moisture stability of **1**.[5]

Initial investigation of the mechanism of ruthenium-mediated olefin metathesis established that the pathway involves substitution of an olefin for phosphine.[6] It was unknown whether olefin binding preceded the loss of phosphine (associative pathway) or phosphine dissociation preceded olefin binding (dissociative pathway). Subsequent kinetic and mechanistic studies showed that the dissociative pathway is the operative mechanism.[7] A complex enters the catalytic cycle (i.e., initiates) by loss of phosphine with a first-order rate constant k_1 (Scheme 1).[8] The resultant 14-electron intermediate **A** can either rebind phosphine (with a rate constant k_{-1}) or bind olefin (with a rate constant k_2). Rebinding of phosphine removes the complex from the catalytic cycle, whereas reaction of **A** with olefin (propagation) continues the catalytic cycle. Intermediate **A** is thus the propagating species. Although neither k_{-1} nor k_2 could be measured directly in solution,[9] the ratios of k_{-1}/k_2 were determined.[7] This ratio of rate constants for phosphine versus olefin binding is a measure of the extent to which a catalyst prefers to remain in the catalytic cycle. Application of the

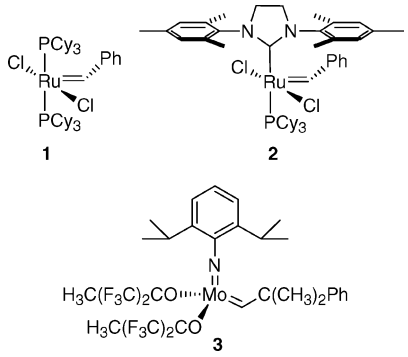

Figure 1. Commercially available catalysts for olefin metathesis.

(1) (a) Ivin, K. J.; Mol, J. C. *Olefin Metathesis and Metathesis Polymerization*; Academic Press: San Diego, CA, 1997. (b) Trnka, T. M.; Grubbs, R. H. *Acc. Chem. Res.* **2001**, *34*, 18. (c) Fürstner, A. *Angew. Chem., Int. Ed.* **2000**, *39*, 3012. (d) Grubbs, R. H.; Chang, S. *Tetrahedron* **1998**, *54*, 4413.
(2) Schwab, P.; Grubbs, R. H.; Ziller, J. W. *J. Am. Chem. Soc.* **1996**, *118*, 100.
(3) (a) Schrock, R. R.; Murdzek, J. S.; Bazan, G. C.; Robbins, M.; Dimare, M.; O'Regan, M. *J. Am. Chem. Soc.* **1990**, *112*, 3875. (b) Schrock, R. R. *Acc. Chem. Res.* **1990**, *23*, 158.
(4) (a) Chatterjee, A. K.; Morgan, J. P.; Scholl, M.; Grubbs, R. H. *J. Am. Chem. Soc.* **2000**, *122*, 3783. (b) Morgan, J. P.; Grubbs, R. H. *Org. Lett.* **2000**, *2*, 3153. (c) Scholl, M.; Ding, S.; Lee, C. W.; Grubbs, R. H. *Org. Lett.* **1999**, *1*, 953. (d) Scholl, M.; Trnka, T. M.; Morgan, J. P.; Grubbs, R. H. *Tetrahedron Lett.* **1999**, *40*, 2247.
(5) (a) Weskamp, T.; Schattenmann, W. C.; Spiegler, M.; Herrmann, W. A. *Angew. Chem., Int. Ed.* **1998**, *37*, 2490. (b) Weskamp, T.; Kohl, F. J.; Hieringer, W.; Gleich, D.; Herrmann, W. A. *Angew. Chem., Int. Ed.* **1999**, *38*, 2416. (c) Huang, J.; Stevens, E. D.; Nolan, S. P.; Peterson, J. L. *J. Am. Chem. Soc.* **1999**, *121*, 2674. (d) Fürstner, A.; Ackermann, L.; Gabor, B.; Goddard, R.; Lehmann, C. W.; Mynott, R.; Stelzer, F.; Thiel, O. R. *Chem. Eur. J.* **2001**, *7*, 3236.
(6) (a) Dias, E. L.; Nguyen, S. T.; Grubbs, R. H. *J. Am. Chem. Soc.* **1997**, *119*, 3887. (b) Ulman, M.; Grubbs, R. H. *Organometallics* **1998**, *17*, 2484.
(7) (a) Sanford, M. S.; Ulman, M.; Grubbs, R. H. *J. Am. Chem. Soc.* **2001**, *123*, 749. (b) Sanford, M. S.; Love, J. A.; Grubbs, R. H. *J. Am. Chem. Soc.* **2001**, *123*, 6543.
(8) For simplicity, this cycle represents a degenerate metathesis reaction.

10.1021/ja027472t CCC: $25.00

Scheme 1

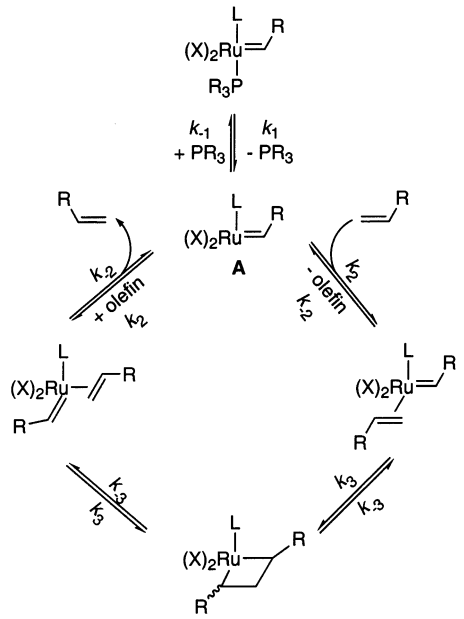

steady-state approximation to the concentration of **A** gives the rate equation shown as eq 1. Whereas initiation of **1** is 2 orders of magnitude faster than that of **2**, the k_{-1}/k_2 ratio of **1** is *4 orders of magnitude greater* than that for **2**, indicating that the rate of metathesis catalyzed by **2** can be up to 2 orders of magnitude greater than that for **1**. Furthermore, complex **2** is capable of reacting with substrates with which **1** either does not react or reacts very slowly, such as electron-deficient and sterically hindered olefins.[10,11] Together, these phenomena account for the overall greater activity of **2** relative to **1**.

$$\text{rate} = k_1k_2[\text{Ru}][\text{olefin}]/\{k_{-1}[\text{PR}_3] + k_2[\text{olefin}]\} \quad (1)$$

Despite the tremendous recent advances in ruthenium-based metathesis catalysts, several issues regarding catalyst initiation remain unsolved. One consequence of low catalyst initiation is that, in many cases, much of the ruthenium complex does not enter the catalytic cycle; the rest is wasted. A recent report noted that in acyclic diene metathesis (ADMET), **2** exhibits higher activity than **1** yet requires higher reaction temperatures due to its lower initiation efficiency.[12] *Increased initiation would permit lower catalyst loadings and reaction temperatures. Improved initiation also has significant implications for metathesis polymerizations*, because initiation efficiency is linked with polymer polydispersities and molecular weights.[13] Control over polydispersity during the ring-opening metathesis polymerization (ROMP) of norbornene has been achieved using catalyst **1** in the presence of excess phosphine.[13a] Phosphine scavengers such as HCl and CuCl have also been utilized to improve initiation of both **1** and **2**, although these additives limit catalyst lifetime and functional group tolerance.[4b,6a,14] An improvement in the inherent initiation ability of a catalyst would preclude these limitations. In particular, *an increase in initiation efficiency, without compromising propagation, would improve the overall catalytic ability of the NHC-bound complexes*. Nolan reported that replacing the PCy_3 of $(IMes)(PCy_3)(Cl)_2Ru{=}CHPh$ with PPh_3 provided an increase in the rate of reaction for the ring-closing metathesis (RCM) of diethyl diallylmalonate.[5c] In a related system, we have demonstrated that the 60-fold improvement in initiation rate obtained by changing the phosphine ligand from PCy_3 to PPh_3 was reflected in a 50-fold increase in reaction rate for the ROMP of cyclooctadiene (COD).[7b] Hoveyda[15] and Blechert[16] have improved initiation by tethering the benzylidene to a weakly associating ligand. However, at this time, there is a poor understanding of the factors that govern initiation rates. We report herein several newly developed, highly efficient ruthenium olefin metathesis catalysts and demonstrate a direct correlation between phosphine electronics and initiation rates.

Results and Discussion

Our previous studies have shown that all of the ancillary ligands impact each of the steps of the metathesis pathway. Improvement of initiation alone does not necessarily lead to a better catalyst, because catalyst activity depends on initiation, phosphine rebinding, reaction of the 14-electron intermediate with olefin, and the rate of catalyst decomposition.[17] This is best illustrated by the differences in activity and initiation between complexes **1** and **2**.[7a] In addition, whereas $(H_2IMes)(PCy_3)(I)_2Ru{=}CHPh$ initiates over 220 times faster than $(H_2IMes)(PCy_3)(Cl)_2Ru{=}CHPh$, the overall activity of these complexes is roughly the same, because propagation (as estimated by the k_{-1}/k_2 ratio) with the diiodide complex is significantly slower than that with the dichloride complex.[7b] In contrast, *NHC-based complexes that differ only by their second neutral ligand all provide the same propagating species upon ligand dissociation* (intermediate A, Scheme 2). In these systems, changing the phosphine affects phosphine dissociation and rebinding, but not the reaction with olefin. Thus, unless phosphine rebinding is also significantly altered, an improvement in initiation should also result in an improvement in the rate of catalysis by increasing the steady-state concentration of the active complex. We therefore examined the effect of different phosphine ligands on initiation, phosphine rebinding, and activity.

(9) For the measurement of k_2 in the gas phase, see: (a) Adlhart, C.; Volland, M. A. O.; Hofmann, P.; Chen, P. *Helv. Chim. Acta* **2000**, *83*, 3306. (b) Adlhart, C.; Chen, P. *Helv. Chim. Acta* **2000**, *83*, 2192. (c) Adlhart, C.; Hinderling, C.; Baumann, H.; Chen, P. *J. Am. Chem. Soc.* **2000**, *122*, 8204. (d) Hinderling, C.; Adlhart, C.; Chen, P. *Angew. Chem., Int. Ed.* **1998**, *37*, 2685.

(10) (a) Choi, T. L.; Chatterjee, A. K.; Grubbs, R. H. *Angew. Chem, Int. Ed.* **2001**, *40*, 1277. (b) See also ref 4a.

(11) (a) Chatterjee, A. K.; Grubbs, R. H. *Org. Lett.* **1999**, *1*, 1751. (b) See also ref 5.

(12) Lehman, S. E.; Wagener, K. B. *Macromolecules* **2002**, *35*, 48.

(13) (a) Bielawski, C. W.; Grubbs, R. H. *Macromolecules* **2001**, *34*, 8838. (b) Robson, D. A.; Gibson, V. C.; Davies, R. G.; North, M. *Macromolecules* **1999**, *32*, 6371.

(14) Photolysis of **1** was found to result in phosphine dissociation. It was suggested that this could be used to initiate ruthenium olefin metathesis catalysts, although such an approach to increasing initiation has not yet been published. Kunkely, H.; Vogler, A. *Inorg. Chim. Acta* **2001**, *325*, 179.

(15) (a) Kingsbury, J. S.; Harrity, J. P. A.; Bonitatebus, P. J., Jr.; Hoveyda, A. H. *J. Am. Chem. Soc.* **1999**, *121*, 791. (b) Garber, S. B.; Kingsbury, J. S.; Gray, B. L.; Hoveyda, A. H. *J. Am. Chem. Soc.* **2000**, *122*, 8168. (c) Van Veldhuizen, J. J.; Garber, S. B.; Kingsbury, J. S.; Hoveyda, A. H. *J. Am. Chem. Soc.* **2002**, *124*, 4954.

(16) (a) Randl, S.; Gessler, S.; Wakamatsu, H.; Blechert, S. *Synlett* **2001**, *3*, 430. (b) Gessler, S.; Randl, S.; Blechert, S. *Tetrahedron Lett.* **2000**, *41*, 9973. (c) Wakamatsu, H.; Blechert, S. *Angew. Chem., Int. Ed.* **2002**, *41*, 794. (d) Wakamatsu, H.; Blechert, S. *Angew. Chem., Int. Ed.* **2002**, *41*, 2403.

(17) Decomposition of complex **1** proceeds through the bimolecular coupling of the 14-electron intermediate. Thus, an increase in initiated complex will increase the decomposition rate. The decomposition of complex **2** is more complicated and several orders of magnitude slower than phosphine dissociation. For a discussion of catalyst decomposition, see: Ulman, M.; Grubbs, R. H. *J. Org. Chem.* **1999**, *64*, 7202.

Scheme 2

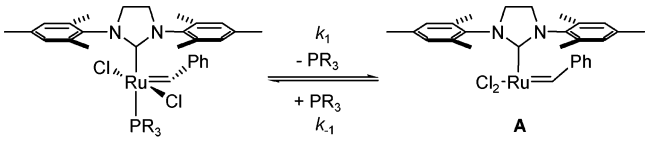

Complex	PR_3	Complex	PR_3
2	PCy_3	**8**	$P(p\text{-}FC_6H_4)_3$
4	$P(n\text{-}Bu)_3$	**9**	$P(C_6H_5)_3$
5	$P(Ph)_2(OMe)$	**10**	$P(p\text{-}CH_3C_6H_4)_3$
6	$P(p\text{-}CF_3C_6H_4)_3$	**11**	$P(p\text{-}CH_3OC_6H_4)_3$
7	$P(p\text{-}ClC_6H_4)_3$		

Scheme 3

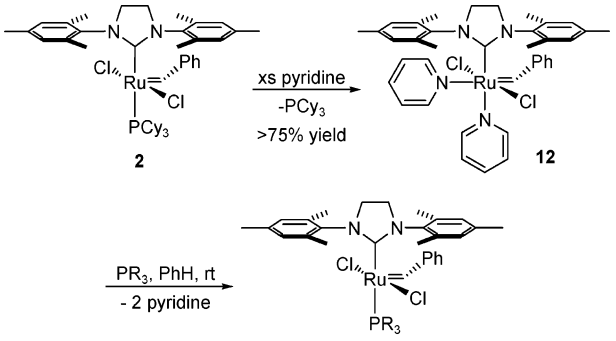

Complex	PR_3	yield
6	$P(p\text{-}CF_3C_6H_4)_3$	51%
7	$P(p\text{-}ClC_6H_4)_3$	70%
8	$P(p\text{-}FC_6H_4)_3$	72%
9	$P(C_6H_5)_3$	73%
10	$P(p\text{-}CH_3C_6H_4)_3$	64%
11	$P(p\text{-}CH_3OC_6H_4)_3$	63%

Synthesis and Structural Characterization. Complexes **6**−**11** are synthesized in two steps from commercially available **2** (Scheme 3); the utility of this protocol has been previously described.[18] Addition of excess pyridine to **2** affords **12**, which is isolated in good yield and with high purity after precipitation, filtration, and washing with pentane. Complexes **6**−**11** are obtained by adding the appropriate phosphine to a solution of bis(pyridine) complex **12** in benzene; these complexes are isolated in good yield and with high purity by removing pyridine in vacuo and washing the solids with pentane. Notably, both steps of this procedure are complete within minutes, are operationally simple (i.e., they can be preformed on the benchtop and using nonpurified solvents), can be performed on a multigram scale, and require only precipitation, filtration, and pentane washes to obtain pure product. Complexes **6**−**11** have been characterized by ^1H, ^{13}C, and ^{31}P NMR spectroscopy and elemental analysis.

Compounds **2**, **7**, and **9** were also characterized by X-ray crystallography.[19] The structures of **2** and **9** are shown in Figures 2 and 3, respectively; the structure of **7** is shown in Supporting Information. Representative bond lengths and bond angles are reported in Table 1. The solid-state structures of complexes **2** and **9** are quite similar, despite containing significantly different phosphine ligands. The Ru−C(1) bond lengths are all within the expected range of similar Ru benzylidenes. In each complex,

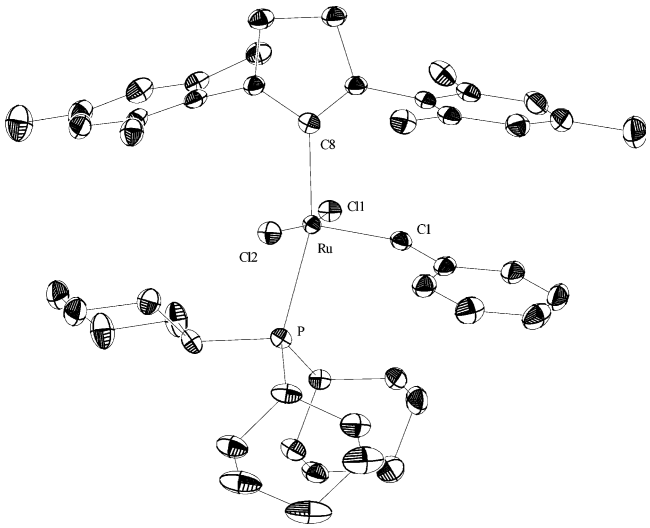

Figure 2. Labeled view of $(H_2IMes)(PCy_3)(Cl)_2Ru{=}CHPh$ (**2**) with 50% probability ellipsoids. Hydrogen atoms have been omitted for clarity.

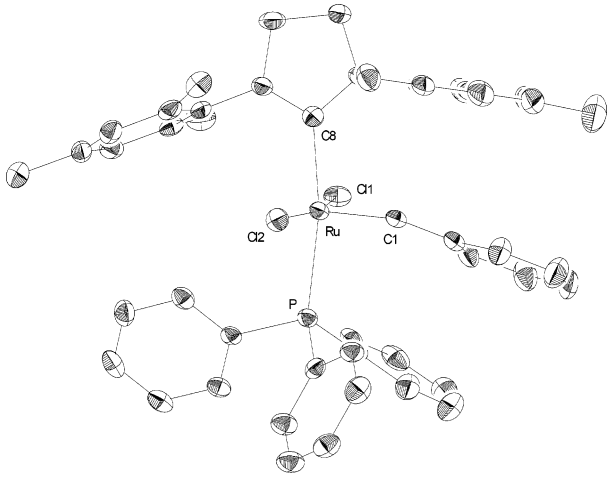

Figure 3. Labeled view of $(H_2IMes)(PPh_3)(Cl)_2Ru{=}CHPh$ (**9**) with 50% probability ellipsoids. Hydrogen atoms have been omitted for clarity.

Table 1. Selected Bond Lengths (Å) and Angles (deg) for Complexes **2** and **9**

bond lengths	complex **2**	complex **9**
Ru−C(1)	1.835(2)	1.847(9)
Ru−C(8)	2.085(2)	2.084(9)
Ru−Cl(1)	2.3988(5)	2.382(3)
Ru−Cl(2)	2.3912(5)	2.392(2)
Ru−P	2.4245(5)	2.404(3)
bond angles	**complex 2**	**complex 9**
C(1)−Ru−C(8)	100.24(8)	98.7(4)
C(1)−Ru−Cl(1)	89.14(7)	102.9(3)
C(1)−Ru−Cl(2)	103.15(7)	90.0(3)
C(8)−Ru−Cl(1)	94.55(5)	83.0(3)
C(8)−Ru−Cl(2)	83.26(5)	93.3(3)
Cl(1)−Ru−Cl(2)	167.71(2)	166.96(9)
C(1)−Ru−P	95.89(6)	93.5(3)
C(8)−Ru−P	163.73(6)	167.1(3)

the Ru−C(8) bond is ∼0.15 Å longer than the Ru−C(1) bond, which is indicative of the greater covalent nature of the Ru-benzylidene bond compared to the Ru-*N*-heterocyclic carbene interaction. The Ru−P bond length of complex **2** is slightly longer (∼0.02 Å) than that for **9**, which correlates inversely with phosphine dissociation rates (vide infra). This is further

(18) Sanford, M. S.; Love, J. A.; Grubbs, R. H. *Organometallics* **2001**, *20*, 5314.
(19) Crystals suitable for X-ray structure determination were obtained by vapor diffusion of pentane into a saturated benzene solution of **2**, **7**, and **9** at room temperature. Crystal data and structure refinement are given in Supporting Information as Table S23.

Table 2. Rate Constants for Phosphine Exchange[a]

complex	PR_3	k_1 (s^{-1}) at 80 °C[b]	k_1 (relative to **2**)	θ (deg)[c]	pK_a[d]
4	$P(n\text{-}Bu)_3$	$[8.1 \pm 0.1] \times 10^{-4}$ [e,f]	0.006	132	8.43
2	PCy_3	0.13 ± 0.01[g]	1.0	170	9.70
5	$P(Ph)_2(OMe)$	1.7 ± 0.4	13	132	2.69
9	PPh_3	7.5 ± 0.6 [f,g]	58	145	2.73

[a] Reactions were carried out in toluene-d_8 with 1 equiv of Ru ([Ru] = 0.04 M) and 1.5 equiv of free PR_3 (relative to bound PR_3). [b] Measured at 80 °C by ^{31}P magnetization transfer unless otherwise specified. [c] Values taken from ref 23. [d] Values taken from ref 20a. [e] Measured by stoichiometric initiation reactions using ethyl vinyl ether, as described in ref 7b. [f] Value for k_1 at 80 °C was extrapolated from an Eyring plot. [g] Values taken from ref 7b.

evidence that the propensity for phosphine dissociation is not reflected in Ru−P bond lengths.[7b]

Initiation. Consistent with our earlier report, both steric and electronic perturbations affect phosphine dissociation. PCy_3 and $P(n\text{-}Bu)_3$ have similar electronics,[20−22] although PCy_3 (cone angle = 170°)[23] dissociates with a rate constant of 0.13 ± 0.01 s^{-1},[24] whereas $P(n\text{-}Bu)_3$ (cone angle = 132°) dissociation could not be measured at the temperatures accessible by NMR magnetization transfer experiments (Table 2). The rate constant for $P(n\text{-}Bu)_3$ dissociation [$(8.1 \pm 0.1) \times 10^{-4}$ s^{-1}] was instead determined using a stoichiometric initiation with ethyl vinyl ether; this technique for measuring initiation has been previously described.[7b] This significant difference in initiation rate can be attributed to the small size of $P(n\text{-}Bu)_3$ relative to PCy_3. However, the rate constant for dissociation of $P(Ph)_2(OMe)$ (cone angle = 132°),[25] is 13 times faster than that for dissociation of PCy_3. In this case, the lower donor strength of $P(Ph)_2(OMe)$ relative to PCy_3 more than compensates for its smaller size. PPh_3 dissociation is the fastest of this series of phosphines, despite its moderate size. From these measurements, we conclude that a weak donor ligand, regardless of steric size, dissociates faster than a stronger electron donor.

The analysis of phosphine electronics is not straightforward; many factors contribute to phosphine donor strength, and this topic continues to be the center of significant debate.[21,22] Choosing any one parameter to represent the electronics of a phosphine is certainly an oversimplification. However, pK_a is typically used as a measure of the σ-donor ability of phosphines coordinated to metals.[22,26] As such, we thought that a correlation might exist between pK_a (or Hammett constant) and phosphine dissociation rate for a series of catalysts containing *para*-substituted triphenylphosphine ligands. These phosphines all have the same cone angle (145°) but differ in their electronic character (Table 3). A plot of Hammett constant σ_p[27,28] versus $\log(k_1)$ shows that a linear free energy relationship does exist between phosphine dissociation rate constant and electronic parameter (Figure 4), with the more electron-poor phosphines dissociating at faster rates than electron-rich phosphines (ρ = 1.7).[29]

Table 3. Parameters for *para*-Substituted Phosphines $[P(p\text{-}XC_6H_4)_3](H_2IMes)(Cl)_2Ru{=}CHPh$[a]

complex	X	k_1 (s^{-1}) at 80 °C	k_1 (rel to **2**)[b]	σ_p[c]	pK_a[d]
6	CF_3	48 ± 2	369	0.53	*e*
7	Cl	17.9 ± 0.4	138	0.23	1.03
8	F	8.5 ± 0.2	65	0.06	1.97
9	H	7.5 ± 0.6 [f,g]	58	0	2.73
10	CH_3	4.1 ± 0.2	32	−0.17	3.84
11	CH_3O	1.8 ± 0.1	14	−0.27	4.57

[a] Reactions were carried out in toluene-d_8 with 1 equiv of Ru ([Ru] = 0.04 M) and 1.5 equiv of free PR_3 (relative to bound PR_3). [b] Measured at 80 °C by ^{31}P magnetization transfer unless otherwise specified. [c] Values taken from ref 27. [d] Values taken from ref 20. [e] Not known. [f] Value taken from ref 7b; see also Table 2. [g] Value for k_1 at 80 °C was extrapolated from an Eyring plot.

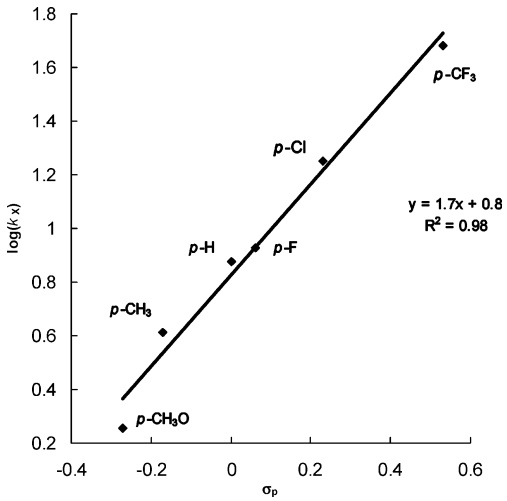

Figure 4. LFER between phosphine dissociation and electronics.

The data in Tables 2 and 3 show that, in general, aryl phosphine dissociation is considerably faster than alkyl phosphine dissociation. Even the slowest of the aryl series (**11**) has an initiation rate constant that is 14 times greater than that for **2**. *Significantly, phosphine dissociation of [P(p-CF3C6H4)3] from complex* ***6*** *is nearly 370 times faster than dissociation of PCy3 from complex* ***2***.[30]

(20) (a) Streuli, C. A. *Anal. Chem.* **1960**, *32*, 985. (b) Allman, T.; Goel, R. G. *Can. J. Chem.* **1982**, *60*, 716.
(21) Assignment of donor strength to phosphines continues to be debated. See: (a) Fernandez, A. L.; Reyes, C.; Wilson, M. R.; Woska, D. C.; Prock, A.; Giering, W. P. *Organometallics* **1997**, *16*, 342. (b) Woska, D. C.; Prock, A.; Giering, W. P. *Organometallics* **2000**, *19*, 4629. (c) Drago, R. S.; Joerg, S. *J. Am. Chem. Soc.* **1996**, *118*, 2654. (d) Joerg, S.; Drago, R. S.; Sales, J. *Organometallics* **1998**, *17*, 589.
(22) Alyea, E. C.; Song, S. *Comments Inorg. Chem.* **1996**, *18*, 189.
(23) Values are for free phosphines. See: Tolman, C. A. *Chem. Rev.* **1977**, *77*, 313.
(24) Values for k_1 were obtained by magnetization transfer experiments, except for complex **4**, which was determined using stoichiometric initiation with ethyl vinyl ether. The magnetization transfer technique is described in further detail in the Experimental Section. The Eyring plot from the initiation experiments with **4** is shown in Supporting Information as Figure S14.
(25) Ascribing a cone angle to an unsymmetrical phosphine is not strictly correct; however, cone angles are the most commonly used method for comparing steric size.
(26) Parameter ^{FT}X, determined from changes in CO stretching frequencies in $Ni(CO)_3L$, has been used as a measure of σ-donor ability, although recent efforts have shown that ^{FT}X does not distinguish between σ-donor and π-back-bonding abilities. See ref 22 for discussion.
(27) Ewing, D. F. In *Correlation Analysis in Chemistry*; Chapman, N. B., Shorter, J., Eds.; Plenum: New York, 1978; pp 357−96.
(28) Hammett constants used in this study are derived from phenol. We feel that these are a better reflection of phosphine pK_a than benzoic acid-derived Hammett constants.
(29) Linear correlation was also obtained by plotting $\log(k_1)$ vs ^{FT}X. This plot is shown in Supporting Information as Figure S13.
(30) Initiation of $[(H_2IMes)(Cl)_2Ru{=}CH(o\text{-}^iPrOC_6H_4)]$ (see refs 15b and 16a,b) was determined to be 6.8 ± 0.8 s^{-1} at 80 °C, using stoichiometric initiation with ethyl vinyl ether, as described in ref 7b. Initiation in this complex presumably proceeds through dissociation of the *iso*-propoxy moiety. Rate constants were measured at four temperatures, and the value at 80 °C was extrapolated from the resulting Eyring plot (Figure S15 in Supporting Information). The rate constants were the same across a range of olefin concentrations (0.17−2.2 M) (Figure S16 in Supporting Information). The lack of dependence of the rate constant on olefin concentration, coupled with the $\Delta S^{\ddagger}$ of ~0 cal mol^{-1} K^{-1}, is consistent with a dissociative mechanism, as is the case with the phosphine-bound complexes.

Table 4. k_{-1}/k_2 Ratios for Complexes **6**−**11**[a]

complex	k_{-1}/k_2	k_{-1} (rel to **2**)[b]
6	7.3	7.0
7	45	36
8	7.9	6.4
9	2.3	1.8
10	2.8	2.2
11	7.5	6.0

[a] Reactions were carried out at 25 °C in toluene-d_8 with [Ru] = 0.017 M. [b] For complex **2**, $k_{-1}/k_2 = 1.25$ at 50 °C (ref 7b).

Scheme 4

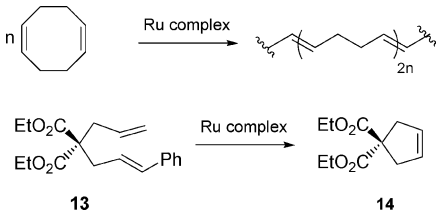

13 **14**

Propagation. Encouraged by the improved initiation rates of complexes **6**−**11** relative to **2**, we next determined the ability of these complexes to remain in the catalytic cycle (as estimated by the ratio of k_{-1}/k_2). We have previously described a method for determining k_{-1}/k_2.[31] The k_{-1}/k_2 values for each complex **6**−**11** are reported in Table 4. This can also be used to obtain relative values of k_{-1} (compared to **2**), since k_2 is the same for all of these complexes.

Somewhat surprisingly, phosphine reassociation does not correlate in a linear fashion with electronics. Equally surprising is that **2** has the lowest k_{-1}/k_2 ratio (1.25) of all of the complexes examined.[32] A possible explanation is that the large size of the PCy_3 ligand could hinder rebinding, thereby biasing the equilibrium toward the 14-electron intermediate. The k_{-1}/k_2 ratio of complex **7** is significantly larger than that for complexes **6** and **8**−**11**, which is inconsistent with a simple correlation between electronics and the rate of phosphine rebinding. Notwithstanding the slightly higher k_{-1}/k_2 ratios of **6**−**11** as compared to **2**, complexes **6**−**11** were still expected to be better catalysts because the increase in k_1 between these catalysts is larger than the corresponding increase in k_{-1}/k_2.

Catalytic Ability. We compared the reactivity of our series of catalysts for two types of metathesis reactions: the ROMP of COD and also RCM of diene **13** (Scheme 4). These reactions were selected because they are representative of processes of interest to the polymer and organic chemistry communities. Furthermore, the ROMP of COD is typically used as a method for comparing catalyst activity.[33] Diene **13** was selected for its ability to regenerate the starting benzylidene (as opposed to methylidene) upon ring closure, which reduces the number of active species in solution and thereby simplifies the kinetic analysis. In addition, RCM substrates with two terminal olefins present an additional challenge in reactions performed in sealed NMR tubes, due to the buildup of ethylene. We had previously noted the less than 2-fold improvement in activity changing from complex **2** to complex **9** for the RCM of diethyl diallyl malonate, when monitoring the reaction by NMR. We attribute this decrease in the relative activity of **9** to the possibility of binding ethylene generated during the reaction.[7b,34] However, ethylene is removed from the reaction under normal metathesis conditions, which reduces the complication of ethylene inhibition. Consequently, the results obtained with **13** are indicative of typical results with other RCM substrates under standard reaction conditions.

Table 5. Activity Comparisons for Complexes **2** and **6**−**11**

complex	k_{rel} polymerization of COD[a]	k_{rel} RCM of **13**[b]
2	1.0	1.0
6	340	7.8
7	95	1.6
8	50	1.7
9	50	3.6
10	20	1.8
11	10	1.7

[a] Reactions were carried out at 20 °C in CD_2Cl_2 with [Ru] = 1 mM, COD:Ru = 1500. [b] Reactions were carried out at 25 °C in CD_2Cl_2 with [Ru] = 5 mM, diene **13**:Ru = 25 (4 mol % Ru).

The relative rates of COD polymerization tend to correlate with the relative rates of initiation (Table 5).[35] *The reaction of COD with complex **6** is 340 times faster than that with **2**.* In comparison, **6** initiates ~370 times faster than **2** (see Tables 2 and 3), suggesting that these systems are near saturation. In fact, all of the ruthenium complexes containing aryl phosphines are more active than **2**. Unlike **2**, complexes **6**−**11** completely initiate during the course of the polymerization (i.e., ^{1}H NMR spectroscopy shows complete conversion of the starting benzylidene to a new alkylidene), as expected on the basis of the measured rates of initiation for these complexes. This suggests that similar reaction rates can be obtained for polymerizations when using considerably less aryl phosphine-based catalyst (in comparison to **2**). A 10-fold increase in the loading of **2** provides similar activity to **11** but remains slower than **6**−**10**. In addition, COD polymerization using **6** is 5 times faster than the phosphine-free catalyst **14** [$(H_2IMes)(Cl)_2Ru{=}CH(o\text{-}^iPrC_6H_4)$].[15,16] The rate of reaction of **14** was measured because past comparisons have been made on the basis of yield of product over time. In our work, we are using kinetic analysis to compare catalyst activity. Complex **14** remains in the catalytic cycle longer, due to the absence of a donor ligand upon initiation. However, **6** ($k_1 = 48 \pm 2$ s^{-1}) is a better initiator than **14** ($k_1 = 6.8 \pm 0.8$ s^{-1})[30] and is therefore more active for the ROMP of COD. *Significantly, the propagating species for complexes **2**−**11** and **14** is identical.* Thus, the relative reaction rates are reflective of the ability of a complex to enter and remain in the catalytic cycle.

The rate differences for the RCM of diene **13** using **6**−**11** compared with **2** are not as dramatic as they are for ROMP, suggesting that the ROMP kinetics are affected primarily by phosphine dissociation, whereas the RCM kinetics are also affected by differences in phosphine rebinding (i.e., the RCM reactions are not at saturation). We chose these reaction conditions because RCM reactions are typically performed at

(31) Method for determining k_{-1}/k_2 is described in the Experimental Section. The rate equation used in data analysis is described in Supporting Information. The assumptions made for this experiment are described in detail in ref 7b.
(32) Since these are ratios of two second-order rate constants, we expect them to be comparable despite the difference in temperature.
(33) (a) Bielawski, C. W.; Grubbs, R. H. *Angew. Chem., Int. Ed.* **2000**, *39*, 2903. (b) Weskamp, T.; Kohl, F. J.; Hieringer, W.; Gliech, D.; Herrmann, W. A. *Angew. Chem., Int. Ed.* **1999**, *38*, 2416. (c) Weskamp, T.; Schattenmann, W. C.; Spiegler, M.; Herrmann, W. A. *Angew. Chem., Int. Ed.* **1998**, *37*, 2490. (d) Dias, E. L.; Grubbs, R. H. *Organometallics* **1998**, *17*, 2758.
(34) Love, J. A.; Grubbs, R. H. Unpublished results.
(35) Notably, the rate constants are reported as relative rate constants.

low concentration (i.e., below saturation) to avoid competing acyclic diene metathesis (ADMET) polymerization reactions. Higher catalyst loadings are often used in RCM to give better rates and higher conversions. In comparison, ROMP reactions are typically performed at substantially lower catalyst loadings and higher monomer concentrations. Significantly, complexes **6**−**11** proved to be more active than **2** for the RCM of diene **13**.[36] The activity of **14** in RCM is similar to the activities of **6**−**11**. The ease of synthesis of complexes **6**−**11** makes these attractive catalysts for olefin metathesis processes. In addition, **6** is an effective RCM catalyst at low catalyst loadings (0.01 mol %). Overall, the aryl−phosphine complexes are faster than **2** for both ROMP and RCM reactions.

Conclusions

We have synthesized and studied a series of *para*-substituted triaryl phosphine-based ruthenium olefin metathesis catalysts. These complexes are readily prepared in two operationally simple, high-yielding steps from commercially available reagents and are air-stable. A linear free energy relationship exists between phosphine σ-donor strength and the rate of catalyst initiation (phosphine dissociation), demonstrating that initiation can be attenuated by tuning phosphine electronics. This is an important consideration for the design of new ruthenium-based metathesis catalysts. These aryl phosphine-based complexes show substantially higher initiation rates than other reported NHC-bound complexes while maintaining high rates of propagation and thus serve as significantly more reactive catalysts for both ROMP and RCM.

Experimental Section

General Procedures. Manipulation of organometallic compounds was performed using standard Schlenk techniques under an atmosphere of dry argon or in a nitrogen-filled Vacuum Atmospheres drybox (O_2 < 2 ppm). NMR spectra were recorded on a Varian Inova instrument (499.85 MHz for ^{1}H; 202.34 MHz for ^{31}P; 125.69 MHz for ^{13}C). ^{1}H and ^{13}C NMR spectra were referenced to the residual solvent. ^{31}P NMR spectra were referenced using H_3PO_4 (δ = 0 ppm) as an external standard. Elemental analyses were performed at Midwest Microlabs (Indianapolis, IN). Mass spectra were recorded on a VG-ZAB mass spectrometer and were carried out at the University of California−Riverside Mass Spectrometry Facility.

Materials and Methods. Pentane, benzene, and benzene-d_6 were dried by passage through solvent purification columns.[37] Toluene-d_8 was dried by vacuum transfer from Na/benzophenone. CD_2Cl_2, pyridine, and ethyl vinyl ether were dried by vacuum transfer from CaH_2 and degassed prior to use. COD was obtained from Aldrich (redistilled, >99% purity) and degassed prior to use. All phosphines were obtained from commercial sources and used as received. Ruthenium complexes **2**, **4**, and **12** were prepared according to literature procedures.[7b] Syntheses of ruthenium complexes **6**, **7**, **9**, and **11** were reported in ref 15 to exemplify the utility of complex **12** as a synthetic precursor to a wide range of previously inaccessible ruthenium complexes; characterization data for these complexes are provided in Supporting Information for completeness. Diene **13** was prepared according to a literature procedure.[38]

(H$_2$IMes)[(*p*-FC$_6$H$_4$)$_3$P](Cl)$_2$Ru=CHPh (8). Complex **12** (200 mg, 0.275 mmol) and (*p*-FC$_6$H$_4$)$_3$P (100 mg, 0.316 mmol) were combined in benzene (2 mL) and stirred for 10 min. The solvent was removed under vacuum, and the resulting brown residue was washed with 5 × 5 mL of pentane and dried under vacuum. Complex **8** was obtained as a pink powder (175 mg, 72% yield). ^{31}P{^{1}H} NMR (CD_2Cl_2): δ 35.70 (m). ^{19}F NMR (CD_2Cl_2): δ −111.08 (m). ^{1}H NMR (CD_2Cl_2): δ 19.15 (s, 1H, Ru=C*H*Ph), 7.41 (d, 2H, ortho C*H*, J_{HH} = 7 Hz), 7.33−7.08 (multiple peaks, 3H, meta and para C*H*), 7.02 (s, 2H, Mes C*H*), 6.94−6.88 (m, 6H, C*H* (*p*-FC$_6$H$_4$)$_3$P), 6.85−6.80 (m, 6H, C*H* (*p*-FC$_6$H$_4$)$_3$P), 6.36 (s, 2H, Mes C*H*), 4.00 (m, 4H, CH_2CH_2), 2.61 (s, 6H, ortho CH_3), 2.43 (s, 3H, para CH_3), 2.23 (s, 6H, ortho CH_3), 1.95 (s, 3H, para CH_3). ^{13}C{^{1}H} NMR (CD_2Cl_2): δ 306.02−305.45 (multiple peaks, Ru = *C*HPh), 218.09 (d, Ru-*C*(N)$_2$, J_{CP} = 92 Hz), 165.23 (d), 163.24 (d), 151.19 (d), 139.68, 138.99, 138.58, 137.42, 136.54 (m), 135.61, 130.77, 130.11 (m), 129.93 (m), 129.66 (m), 128.06, 127.99 (m), 126.80 (d), 126.47 (d), 115.40 (m), 52.53 (d), 51.82 (d), 21.51 (m), 21.18 (m), 20.47 (m), 18.73 (m). Anal. Calcd for $C_{46}H_{44}N_2F_3Cl_2PRu$: C, 62.44; H, 5.01; N, 3.17. Found: C, 62.64; H, 5.03; N, 3.13.

(H$_2$IMes)[(*p*-MeC$_6$H$_4$)$_3$P](Cl)$_2$Ru=CHPh (10). Complex **12** (200 mg, 0.275 mmol) and (*p*-MeC$_6$H$_4$)$_3$P (90 mg, 0.296 mmol) were combined in benzene (2 mL) and stirred for 10 min. The solvent was removed under vacuum, and the resulting brown residue was washed with 5 × 5 mL of pentane and dried under vacuum. Complex **10** was obtained as a pink powder (155 mg, 64% yield). ^{31}P{^{1}H} NMR (CD_2Cl_2): δ 35.26 (s). ^{1}H NMR (CD_2Cl_2): δ 19.15 (s, 1H, Ru=C*H*Ph), 7.39 (d, 2H, ortho C*H*, J_{HH} = 7.5 Hz), 7.28 (t, 1H, para C*H*, J_{HH} = 7.5 Hz), 7.16 (m, 2H, meta C*H*), 7.03 (s, 2H, Mes C*H*), 6.89 (m, 6H, C*H* (*p*-MeC$_6$H$_4$)$_3$P), 6.78 (m, 6H, C*H* (*p*-MeC$_6$H$_4$)$_3$P), 6.35 (s, 2H Mes C*H*), 4.00 (m, 4H, CH_2CH_2), 2.62 (s, 6H, ortho CH_3), 2.44 (s, 6H, ortho CH_3), 2.28 (s, 9H, CH_3 (*p*-MeC$_6$H$_4$)$_3$P), 2.22 (s, 3H, para CH_3), 1.96 (s, 3H, para CH_3). ^{13}C{^{1}H} NMR (CD_2Cl_2): δ 305.90 (m, Ru = *C*HPh), 212.24 (d, Ru-*C*(N)$_2$, J_{CP} = 90 Hz), 151.12 (m), 140.01, 138.78, 138.36, 137.45, 134.37 (d), 132.46, 132.38, 130.91, 130.12, 129.62, 129.25, 128.80, 128.76, 128.20, 127.87, 127.80, 52.55 (d, J_{CP} = 4 Hz), 51.80 (d, J_{CP} = 2 Hz), 21.65, 21.58, 20.47, 18.77. Anal. Calcd for $C_{49}H_{53}N_2Cl_2PRu$: C, 67.42; H, 6.12; N, 3.21. Found: C, 67.70; H, 6.18; N, 2.81.

Magnetization Transfer Experiments. The ruthenium alkylidene (0.024 mmol) and P(*p*-XC$_6$H$_4$)$_3$ (in equivalents relative to [Ru]) were combined in toluene-d_8 (600 μL) in an NMR tube, and the resulting solution was allowed to thermally equilibrate in the NMR probe. The free phosphine resonance was selectively inverted using the DANTE pulse sequence,[39] and after variable mixing times (between 0.00003 and 50 s), a nonselective 90° pulse was applied and an FID recorded. ^{1}H decoupling was applied during the 90° pulse. Spectra were collected as 4−8 transients with relaxation delays of 50 s. The peak heights of the free and bound phosphine at variable mixing times were analyzed using the computer program CIFIT[40] in order to obtain the exchange rate of bound phosphine with free phosphine (k_1). The relaxation time (T_1) values for the free and bound phosphine were also obtained in this analysis, and the results are summarized in Table S1 in Supporting Information. T_1 values for complexes **6**−**11** as well as for the free phosphines were determined independently using standard inversion recovery experiments, and the results are summarized in Table S2 in Supporting Information. Nonlinear least-squares fits for catalysts **6**−**11** are shown in Figure S1 in Supporting Information. Values for activation parameters for complexes **6**−**11**, obtained from the Eyring plots, are summarized in Table S3 in Supporting Information.

NMR Initiation Kinetics (for 4 and 14). The ruthenium alkylidene (0.0106 mmol) was dissolved in toluene-d_8 (600 μL) in an NMR tube fitted with a screw cap containing a rubber septum. The resulting solution was allowed to equilibrate in the NMR probe at the appropriate temperature, and ethyl vinyl ether (in equivalents relative to [Ru]) was injected into the NMR tube neat. Reactions were monitored by measuring the peak heights of the starting alkylidene as a function of

(36) Rate of reaction using complex **9** increases linearly with concentration of **13**.
(37) Pangborn, A. B.; Giardello, M. A.; Grubbs, R. H.; Rosen, R. K.; Timmers, F. J. *Organometallics* **1996**, *15*, 1518.
(38) Hanessian, S.; Leger, R. *J. Am. Chem. Soc.* **1992**, *114*, 3115. See also: Kirkland, T. A.; Lynn, D. M.; Grubbs, R. H. *J. Org. Chem.* **1998**, *63*, 9904.
(39) Morris, G. A.; Freeman, R. *J. Magn. Res.* **1978**, *29*, 433.
(40) Bain, A. D.; Kramer, J. A. *J. Magn. Res.* **1996**, *118A*, 21.

time over at least three half-lives. The data were fitted to a first-order exponential using Varian kinetics software.[41]

$1/k_{obs}$ versus [PR_3]/[Olefin]. Ruthenium catalyst (0.0106 mmol) and PR_3 (in equivalents relative to [Ru]) were combined in an NMR tube fitted with a screw cap containing a rubber septum. The solids were dissolved in 600 μL of toluene-d_8. Each solution was allowed to thermally equilibrate in the NMR probe at 25 °C, and ethyl vinyl ether (15 μL) was injected neat into the NMR tube. Reactions were monitored by measuring the peak heights of the starting alkylidene as a function of time over five half-lives. The data were fitted to a first-order exponential using Varian kinetics software.[41] The rate equation used for analysis is described in Supporting Information. Plots of $1/k_{obs}$ as a function of [PR_3]/[olefin] for complexes **6**−**11** are shown in Figures S2−S7. Estimates of k_1 (determined from the intercept of the plots) are tabulated in Table S4.

ROMP of Cyclooctadiene: Comparison of 2 and 6−11. The ruthenium alkylidene (0.0006 mmol) was dissolved in CD_2Cl_2 (600 μL) in an NMR tube fitted with a screw cap containing a rubber septum. The resulting solution was allowed to equilibrate in the NMR probe at 20 °C, and COD (110 μL, 0.90 mmol, 1.5 M) was injected into the NMR tube neat. Reactions were monitored by measuring the peak heights of the COD olefinic signal as a function of time over five half-lives. The data were fitted to a first-order exponential using Varian kinetics software.[41] **Comparison of 6 and 14.** The ruthenium alkylidene (0.0003 mmol) was dissolved in CD_2Cl_2 (600 μL) in an NMR tube fitted with a screw cap containing a rubber septum. The resulting solution was allowed to equilibrate in the NMR probe at 10 °C, and COD (110 μL, 0.90 mmol, 1.5 M) was injected into the NMR tube neat. The reactions were monitored and analyzed as described above.

RCM of Diene 13. The ruthenium alkylidene (0.003 mmol) was dissolved in CD_2Cl_2 (600 μL) in an NMR tube fitted with a screw cap containing a rubber septum. The resulting solution was allowed to equilibrate in the NMR probe at 25 °C, and **13** (25 mg, 0.13 M) was injected into the NMR tube neat. Reactions were monitored by measuring the peak heights of the allylic methylene signals of **13** as a function of time over five half-lives. The data were fitted to a first-order exponential using Varian kinetics software.[41]

(41) *VNMR 6.1B Software*; Varian Associates, Inc.: Palo Alto, CA, 2001.

X-ray Crystal Structures of 2, 7, and 9. Crystal, intensity collection, and refinement details[42] are summarized in Supporting Information as Table S23. In each case, the selected crystal was mounted on a glass fiber with Paratone-N oil and transferred to a Bruker SMART 1000 CCD area detector equipped with a Crystal Logic CL24 low-temperature device. Data were collected with ω-scans at seven φ values and subsequently processed with SAINT.[43] No absorption or decay corrections were applied. SHELXTL[43] was used to solve (by direct methods and subsequent difference Fourier maps) and refine (full-matrix least-squares on F^2) the structure. All non-hydrogen atoms were refined anisotropically; the hydrogen atoms were placed at calculated positions with U_{iso} values based on the U_{eq} of the attached atom. Pertinent bond lengths and angles for **2** and **9** are presented in Table 1.

Acknowledgment. The authors would like to thank Lawrence M. Henling (X-ray crystallography), Tina M. Trnka, John P. Morgan, and D. William Ward for helpful discussions and Materia, Inc., for a generous supply of complex **2**. J.A.L. thanks the National Institutes of Health for a postdoctoral fellowship. This work was supported by the National Science Foundation.

Supporting Information Available: Experimental data for the synthesis of all new complexes, tables of phosphine exchange rate constants, T_1 data, Eyring plots, activation parameters, rate equations, $1/k_{obs}$ versus [PR_3]/[olefin] plots, and crystallographic data (labeled drawings, table of atomic coordinates, complete bond distances and angles, and anisotropic displacement parameters) for complexes **2**, **7**, and **9**. This material is available free of charge via the Internet at http://pubs.acs.org.

JA027472T

(42) Crystallographic information files (CIFs) for **2**, **7**, and **9** have been deposited with the Cambridge Crystallographic Data Centre as supplementary publication nos. CCDC 161995, 174072, and 167560, respectively. These data can be obtained free of charge via http://www.ccdc.cam.ac.uk/conts/retrieving.html (or from the Cambridge Crystallographic Data Centre, 12, Union Road, Cambridge CB2 1EZ, UK. Fax: +44 1223 336033. E-mail: deposit@ccdc.cam.ac.uk). Structure factors are available from the authors via e-mail: xray@caltech.edu.

(43) *SMART*, *SAINT*, and *SHELXTL*; Bruker AXS, Inc.: Madison, WI, 1999.